A UTD Solution for the Scattering by a Wedge with Anisotropic Impedance Faces: Skew Incidence Case

Giuseppe Pelosi, *Senior Member, IEEE*, Giuliano Manara, *Senior Member, IEEE*, and Paolo Nepa, *Member, IEEE*

***Abstract*— Asymptotic expressions for the fields scattered by an anisotropic impedance wedge at oblique incidence are derived in the context of the uniform geometrical theory of diffraction (UTD). They are obtained by resorting to a perturbative approach, considering the normal incidence case as the imperturbed configuration. We observe that the limits of applicability of this approximate analytical solution extend far beyond those of standard perturbative approaches, allowing us to account for deviations from the normal incidence case of 20° to 30°.**

***Index Terms*— Electromagnetic scattering, geometrical theory of diffraction, tropic surfaces.**

I. Introduction

In the design of high-frequency antennas and in radar cross section (RCS) predictions, an important canonical problem is constituted by plane wave scattering from wedge-type configurations with arbitrary anisotropic impedance boundary conditions (IBC's) on their faces. At oblique incidence, with the exception of some specific configurations, this electromagnetic scattering problem has not yet been solved analytically. Solutions presented in the literature are based either on numerical approaches [1]–[3] or on analytical techniques, but in this latter case, they are limited to specific configurations [4]–[11].

The main purpose of this paper is to provide suitable diffraction coefficients in the format of the uniform geometrical theory of diffraction (UTD) [12] for describing plane wave scattering from an anisotropic impedance wedge with an arbitrary exterior angle at oblique incidence when the impedance tensor on the two faces of the wedge has its principal axes parallel and perpendicular to the edge of the wedge. We note that more general impedance tensors have been taken into account only in [4], [7], and [8] for the normal incidence case and in [1] for oblique incidence.

First, Sommerfeld-type approximate integral representations for the longitudinal components of the total field are determined. This is accomplished by resorting to a perturbative expansion with respect to the cosine of the incidence skewness angle, taking into account all terms up to the second order. The procedure followed, which is an extension of that suggested in [4], [7], [8], [13], is based on the Maliuzhinets method [14]. Then, these integral representations are asymptotically evaluated in the framework of the UTD, taking also into account the presence of complex poles (surface wave poles).

The paper has been organized as follows. The problem is formulated in Section II, and suitable approximate integral representations for the longitudinal components of the fields are provided in Section III. Then, analytical expressions for the residue contributions related to the geometrical optics (GO) field and the surface waves are given in Section IV, where the asymptotic evaluation of the diffraction integral is also performed in the context of UTD to provide a matrix diffraction coefficient. Finally, samples of numerical results are presented in Section V and compared with those obtained by resorting to numerical [2] and rigorous analytical solutions [9], [10], [15] available in the literature, in order to test the accuracy of this perturbative technique and define its limits of applicability.

Finally, it is worth observing that this solution can be applied to the case of the isotropic impedance wedge as well, extending the class of available analytical solutions for three-dimensional (3-D) electromagnetic scattering (see, for example, [15]) to more general configurations with arbitrary impedance faces and arbitrary exterior wedge angles, although in the limits of accuracy of this perturbative approach.

II. Formulation of the Problem

The 3-D geometry for the scattering problem is depicted in Fig. 1. The wedge has its edge along the z axis of a cylindrical reference frame—a harmonic plane wave with an arbitrary polarization impinges on the edge from a direction determined by the two angles β' and ϕ'. β' is a measure of the incidence direction skewness with respect to the edge of the wedge: $\beta' = \pi/2$ corresponds to normal incidence. An $\exp(j\omega t)$ time dependence is assumed and suppressed.

In particular, the longitudinal components of the incident field can be expressed as

$$[E_z^i,\, \zeta_0 H_z^i] = [e_z,\, h_z] e^{-jkz\,\cos\,\beta'} e^{jk\rho\,\sin\,\beta'\,\cos(\phi-\phi')} \quad (1)$$

where ζ_0 and k are the free-space intrinsic impedance and wavenumber, respectively. The observation point is at P and the exterior wedge angle is $n\pi$. Two different anisotropic IBC's hold on the two faces and are represented by the tensors $\overline{\overline{Z}}_{0,n} = (Z_{0,n})_z \hat{z}\hat{z} + (Z_{0,n})_\rho \hat{\rho}\hat{\rho}$. Consequently, the IBC's are expressed as [5]

$$E_\rho = (Z_0)_\rho H_z, \quad E_z = -(Z_0)_z H_\rho \qquad \phi = 0 \quad (2a)$$

$$E_\rho = -(Z_n)_\rho H_z, \; E_z = (Z_n)_z H_\rho \qquad \phi = n\pi \quad (2b)$$

with $\Re[(Z_{0,n})_{z,\rho}] \geq 0$.

Manuscript received June 25, 1997; revised November 7, 1997.

G. Pelosi is with the Department of Electronic Engineering, University of Florence, I-50134 Florence, Italy.

G. Manara and P. Nepa are with the Department of Information Engineering, University of Pisa, I-56126 Pisa, Italy.

Publisher Item Identifier S 0018-926X(98)02686-6.

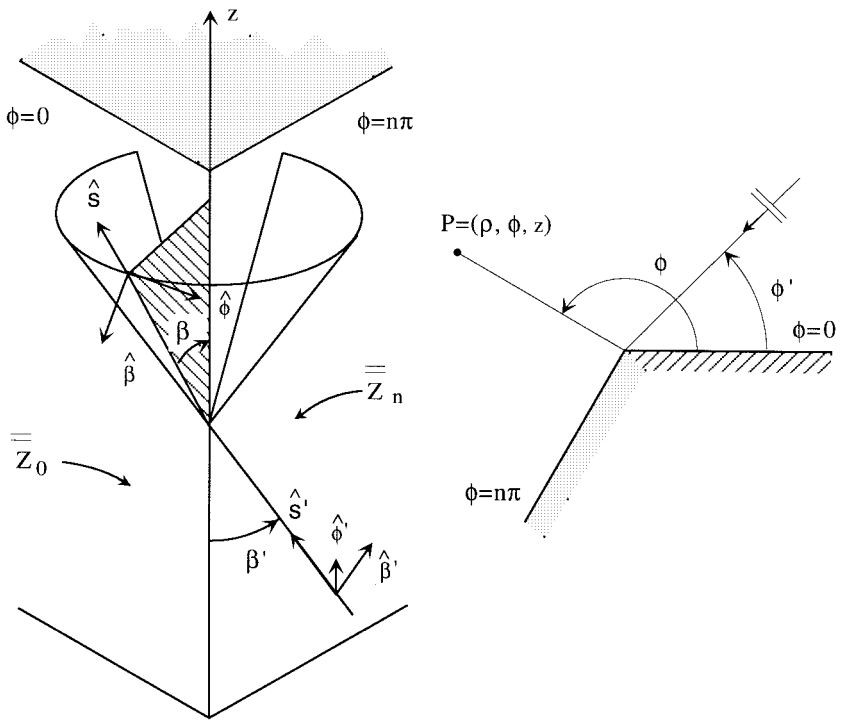

Fig. 1. Geometry for the diffraction at a wedge with anisotropic impedance faces.

The electric properties of the wedge are supposed to be independent of z, consequently, all field components contain a common z-dependence factor $\exp(-jkz\cos\beta')$ that will be suppressed in the following. Moreover, all field components transverse to the z axis can be represented in terms of $[E_z, \zeta_0 H_z]$. The total field longitudinal components $[E_z, \zeta_0 H_z]$ are solutions of the Helmholtz equation $(\nabla_t^2 + k_t^2)[E_z, \zeta_0 H_z] = 0$, with $k_t = k\sin\beta'$, and must satisfy the radiation and edge conditions. By expressing the IBC's in (2) in terms of $[E_z, \zeta_0 H_z]$, we obtain

$$\frac{1}{\rho}\frac{\partial E_z}{\partial \phi} + jk_t\epsilon_{0,n}\sin\beta'\sin\theta^e_{0,n}E_z - \cos\beta'\frac{\partial(\zeta_0 H_z)}{\partial\rho} = 0, \qquad \phi = 0,\ n\pi \tag{3a}$$

$$\frac{1}{\rho}\frac{\partial(\zeta_0 H_z)}{\partial \phi} + jk_t\epsilon_{0,n}\sin\beta'\sin\theta^h_{0,n}(\zeta_0 H_z) + \cos\beta'\frac{\partial E_z}{\partial\rho} = 0, \qquad \phi = 0,\ n\pi \tag{3b}$$

where $\epsilon_0 = -1$ and $\epsilon_n = +1$. In (3), $\sin\theta^e_{0,n} = \zeta_0/(Z_{0,n})_z$ and $\sin\theta^h_{0,n} = (Z_{0,n})_\rho/\zeta_0$ define the Brewster angles $\theta^e_{0,n}$ and $\theta^h_{0,n}$ of the $\phi = 0$ and $\phi = n\pi$ face of the wedge for perpendicular and parallel polarizations [14], respectively. The longitudinal components of the total electric and magnetic fields can be expressed [14] by the following integral representations:

$$E_z(\rho,\phi) = \frac{1}{2\pi j}\int_\gamma f(\alpha+\phi-n\pi/2)e^{jk_t\rho\cos\alpha}\,d\alpha \tag{4a}$$

$$\zeta_0 H_z(\rho,\phi) = \frac{1}{2\pi j}\int_\gamma s(\alpha+\phi-n\pi/2)e^{jk_t\rho\cos\alpha}\,d\alpha \tag{4b}$$

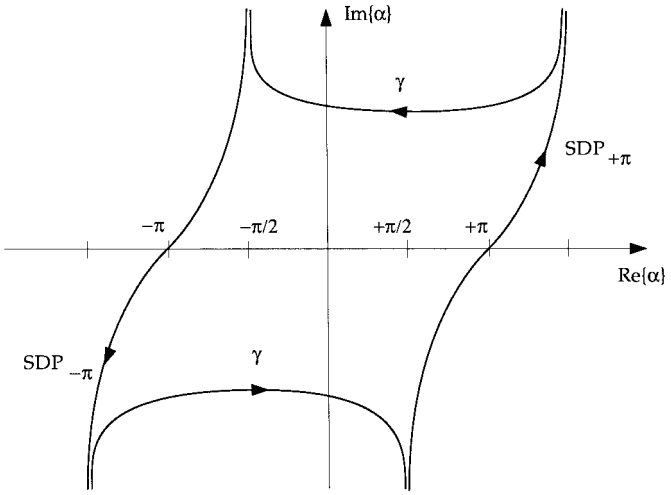

Fig. 2. Integration paths in the complex plane.

where γ is the Sommerfeld integration path (Fig. 2) and the spectral functions $[f, s]$ verify the inequalities $|[f(\alpha), s(\alpha)] - [f(\pm j\infty), s(\pm j\infty)]| < \exp[-c|\Im(\alpha)|]$, $c > 0$, in the limit for $\Im(\alpha) \to \pm\infty$ inside the strip $|\Re(\alpha)| \le n\pi/2$, in agreement with the edge condition [16]. In the same strip, $[f, s]$ must be regular, except for first-order pole singularities at $\alpha = \phi' - n\pi/2$, which account for the incident field.

III. Derivation of the Spectral Functions

After substituting the integral representations in (4) into the IBC's in (3), two integral equations are obtained for each face. Taking into account that the IBC's considered here are of the first order and applying the Maliuzhinets theorem [16], the

following set of functional equations is obtained:

$$\begin{aligned}&(\sin\alpha+\epsilon_{0,n}\sin\beta'\sin\theta^e_{0,n})f(\alpha+\epsilon_{0,n}n\pi/2)\\&\quad+(\sin\alpha-\epsilon_{0,n}\sin\beta'\sin\theta^e_{0,n})f(-\alpha+\epsilon_{0,n}n\pi/2)\\&\quad=\cos\alpha\cos\beta'\{s(\alpha+\epsilon_{0,n}n\pi/2)\}\\&\quad\quad-s(-\alpha+\epsilon_{0,n}n\pi/2)]\end{aligned}\tag{5a}$$

$$\begin{aligned}&(\sin\alpha+\epsilon_{0,n}\sin\beta'\sin\theta^h_{0,n})s(\alpha+\epsilon_{0,n}n\pi/2)\\&\quad+(\sin\alpha-\epsilon_{0,n}\sin\beta'\sin\theta^h_{0,n})s(-\alpha+\epsilon_{0,n}n\pi/2)\\&\quad=-\cos\alpha\cos\beta'\{f(\alpha+\epsilon_{0,n}n\pi/2)\\&\quad\quad-f(-\alpha+\epsilon_{0,n}n\pi/2)\}.\end{aligned}\tag{5b}$$

In the framework of a perturbative technique and for small deviations from the normal incidence condition ($|\cos\beta'|\ll 1$), we seek an expression for the unknown spectral functions in the following form considering only terms up to second order (see Appendix A):

$$\begin{aligned}f(\alpha)&\simeq e_z f_0(\alpha)+h_z f_1(\alpha)\cos\beta'\\&\quad+e_z f_2(\alpha)\cos^2\beta'\end{aligned}\tag{6a}$$

$$\begin{aligned}s(\alpha)&\simeq h_z s_0(\alpha)+e_z s_1(\alpha)\cos\beta'\\&\quad+h_z s_2(\alpha)\cos^2\beta'.\end{aligned}\tag{6b}$$

Substituting (6) into (5) and equating the coefficients of the various powers of $\cos\beta'$ individually, a system of functional equations is obtained for $[f_i,\, s_i]$ and $i=0,\,1,\,2$. In particular, f_0 and s_0 are the spectral functions corresponding to the diffraction of a unit amplitude plane wave impinging on the edge at normal incidence with $\mathrm{TM}_z(e)$ and $\mathrm{TE}_z(h)$ polarizations, respectively [14]

$$\begin{aligned}[f_0(\alpha),\, s_0(\alpha)]=[&\Psi^e(\alpha)/\Psi^e(\phi'-n\pi/2),\\&\Psi^h(\alpha)/\Psi^h(\phi'-n\pi/2)]\sigma(\alpha).\end{aligned}\tag{7}$$

$\Psi^e(\alpha)=\Psi(\alpha,\,\theta^e_0,\,\theta^e_n)$ and $\Psi^h(\alpha)=\Psi(\alpha,\,\theta^h_0,\,\theta^h_n)$ contain the Maliuzhinets special function and are defined in [14] (see also [17, Appendix B.4]). $\Psi^e(\alpha)$ and $\Psi^h(\alpha)$ are meromorphic functions which are regular in the strip $|\mathrm{Re}(\alpha)|\le n\pi/2$ and exhibit first-order pole singularities at $\alpha=\epsilon_{0,n}(\alpha+n\pi/2+\theta^e_{0,n})$ and $\alpha=\epsilon_{0,n}(\alpha+n\pi/2+\theta^h_{0,n})$, respectively. The corresponding residues provide the contributions to the field due to the surface waves supported by the wedge faces, when they exist. Moreover

$$\sigma(\alpha)=\frac{1}{n}\frac{\sin(\phi'/n)}{\sin(\alpha/n)+\cos(\phi'/n)}\tag{8}$$

shows first-order pole singularities accounting for the GO field. $[f_1,\, s_1]$ satisfy inhomogeneous functional equations of the Maliuzhinets type

$$f_1(\alpha^+_{0,n})+R^e_{0,n}(\alpha)f_1(\alpha^-_{0,n})=L_{0,n}(\alpha,\,\theta^e_{0,n};\,s_0)\tag{9a}$$

$$s_1(\alpha^+_{0,n})+R^h_{0,n}(\alpha)s_1(\alpha^-_{0,n})=-L_{0,n}(\alpha,\,\theta^h_{0,n};\,f_0)\tag{9b}$$

where $\alpha^+_{0,n}=\epsilon_{0,n}(\alpha+n\pi/2)$, $\alpha^-_{0,n}=\epsilon_{0,n}(-\alpha+n\pi/2)$ and

$$R^e_{0,n}(\alpha)=\frac{\sin\alpha-\sin\theta^e_{0,n}}{\sin\alpha+\sin\theta^e_{0,n}}\tag{10a}$$

$$R^h_{0,n}(\alpha)=\frac{\sin\alpha-\sin\theta^h_{0,n}}{\sin\alpha+\sin\theta^h_{0,n}}\tag{10b}$$

are the generalized reflection coefficients for the $\phi=0$ and $\phi=n\pi$ face, respectively. Moreover, in (9a) and (9b)

$$\begin{aligned}L_{0,n}(\alpha,\,\theta_{0,n};\,t)=\epsilon_{0,n}&\frac{\cos\alpha}{\sin\alpha+\sin\theta_{0,n}}\\&\cdot[t(\alpha^+_{0,n})-t(\alpha^-_{0,n})].\end{aligned}\tag{11}$$

Similar inhomogeneous functional equations hold for $[f_2,\, s_2]$

$$\begin{aligned}&f_2(\alpha^+_{0,n})+R^e_{0,n}(\alpha)f_2(\alpha^-_{0,n})\\&\quad=L_{0,n}(\alpha,\,\theta^e_{0,n};\,s_1)+\epsilon_{0,n}\frac{\sin\theta^e_{0,n}}{2\cos\alpha}L_{0,n}(\alpha,\,\theta^e_{0,n};\,f_0)\end{aligned}\tag{12a}$$

$$\begin{aligned}&s_2(\alpha^+_{0,n})+R^h_{0,n}(\alpha)s_2(\alpha^-_{0,n})\\&\quad=-L_{0,n}(\alpha,\,\theta^h_{0,n};\,f_1)+\epsilon_{0,n}\frac{\sin\theta^h_{0,n}}{2\cos\alpha}L_{0,n}(\alpha,\,\theta^h_{0,n};\,s_0)\end{aligned}\tag{12b}$$

where the second member is again known, once the functional equations in (9) have been solved.

The solution of inhomogeneous functional equations of the Maliuzhinets type as those in (9) and (12) has been given by Tuzhilin in [18] (see also [7] and [8]) in a form involving special integral functions defined along an integration path coinciding with the imaginary axis of the complex plane. $[f_1,\, s_1]$ and $[f_2,\, s_2]$ are expressed as

$$[f_1(\alpha),\, s_1(\alpha)]=[\Psi^e(\alpha)\tau_1(\alpha),\,\Psi^h(\alpha)\sigma_1(\alpha)]\tag{13a}$$

$$[f_2(\alpha),\, s_2(\alpha)]=[\Psi^e(\alpha)\tau_2(\alpha),\,\Psi^h(\alpha)\sigma_2(\alpha)]\tag{13b}$$

where $\Psi^e(\alpha)$ and $\Psi^h(\alpha)$ have been defined above. Explicit integral expressions for the meromorphic functions $\tau_{1,2}$ and $\sigma_{1,2}$ are given in Appendix B. It is worth noting that $[\tau_{1,2},\,\sigma_{1,2}]$ are regular in the strip $|\mathrm{Re}(\alpha)|\le n\pi/2$, since the pole singularities providing the contribution of the incident field have been already accounted for in $[f_0,\, s_0]$.

IV. UTD Solution

Introducing (6) into (4), the longitudinal components of the total field $[E_z,\,\zeta_0 H_z]$ are expressed in the form of a summation of Sommerfeld integrals as

$$\begin{aligned}[E_z,\,\zeta_0 H_z]&\simeq\sum_{m=0}^{2}[E_z,\,\zeta_0 H_z]_m\\&=\frac{1}{2\pi j}\int_\gamma[e_z f_0,\,h_z s_0]e^{jk_t\rho\cos\alpha}\,d\alpha\\&\quad+\cos\beta'\frac{1}{2\pi j}\int_\gamma[h_z f_1,\,e_z s_1]e^{jk_t\rho\cos\alpha}\,d\alpha\\&\quad+\cos^2\beta'\frac{1}{2\pi j}\int_\gamma[e_z f_2,\,h_z s_2]e^{jk_t\rho\cos\alpha}\,da.\end{aligned}\tag{14}$$

By applying the residue theorem, all the above integral representations defined along the Sommerfeld integration contour γ are reduced to the contribution of: 1) two integrals, defined along the steepest descent paths $(\mathrm{SDP})_{\pm\pi}$ through the saddle points at $\pm\pi$ (see Fig. 2) and 2) the residues of the poles of $[f_m,\, s_m]$, $m=0,\,1,\,2$, internal to the closed contour formed

by γ and the SDP$_{\pm\pi}$. The integrals along the SDP$_{\pm\pi}$ provide the contribution to the total field due to the diffraction by the edge. A uniform high-frequency approximation for the zeroth-order field contribution $[E_z,\, \zeta_0 H_z]_0$ has been performed in [19] in the context of the UTD [12]. As apparent from the first integral term in (14), the large parameter $k\rho$ in the asymptotic evaluation in [19] must be replaced by $k_t\rho$. The asymptotic evaluation of the higher order contributions to the field, namely, the second and third term in (14), will be discussed in detail in this section.

A. Residue Contributions

The spectral functions $[f_m(\alpha),\, s_m(\alpha)] = [\Psi^e(\alpha)\tau_m(\alpha),\, \Psi^h(\alpha)\sigma_m(\alpha)]$ $(m = 1, 2)$ exhibit two different kinds of poles, which will be classified in the following as: 1) geometrical poles (their residues provide the correction to the reflected field contribution) and 2) electric poles (their residues provide the correction to the surface wave contribution). In particular, the electric poles in 2) give a contribution only when the two faces of the wedge can support surface wave propagation. The conditions for which the residues of the poles in 2) must be included in the asymptotic solution coincide with the corresponding conditions for the poles related to the surface wave contributions in $[E_z,\, \zeta_0 H_z]_0$.

Explicit expressions for the residues are given next.

1) Geometrical Poles: The locations of the geometrical poles on the complex α plane are

$$\alpha = \alpha_1 = \alpha_{0,n}^{go} = -\phi + n\pi/2 + \epsilon_{0,n}(n\pi/2 + \xi_{0,n}) \tag{15}$$

where

$$\xi_{0,n} = n\pi/2 + \epsilon_{0,n}(-\phi' + n\pi/2). \tag{16}$$

Explicit expressions for the residue contributions are

$$\begin{aligned}&\mathrm{Res}\{f_1(\alpha+\phi-n\pi/2)e^{jk_t\rho\,\cos\,\alpha},\ \alpha=\alpha_{0,n}^{go}\}\\ &\quad=\epsilon_{0,n}\,\cos\,\xi_{0,n}\{1+R_{0,n}^{e}(\xi_{0,n})\}\,\frac{e^{jk_t\rho\,\cos\,\alpha_{0,n}^{go}}}{\sin\,\xi_{0,n}+\sin\,\theta_{0,n}^{h}}\end{aligned} \tag{17}$$

$$\begin{aligned}&\mathrm{Res}\{s_1(\alpha+\phi-n\pi/2)e^{jk_t\rho\,\cos\,\alpha},\alpha=\alpha_{0,n}^{go}\}\\ &\quad=-\epsilon_{0,n}\,\cos\,\xi_{0,n}\{1+R_{0,n}^{h}(\xi_{0,n})\}\,\frac{e^{jk_t\rho\,\cos\,\alpha_{0,n}^{go}}}{\sin\,\xi_{0,n}+\sin\,\theta_{0,n}^{e}}.\end{aligned} \tag{18}$$

They must be included in the asymptotic solution only when $0 < (\epsilon_{0,n}+1)n\pi/2 - \epsilon_{0,n}\phi < \pi - \xi_{0,n}$. It is important to note that the residue expressions in (17) and (18) coincide with the first derivative with respect to $\cos\,\beta'$ of the off-diagonal terms in the reflection matrix of the corresponding face of the anisotropic wedge, evaluated at $\beta' = \pi/2$. This reflection matrix can be easily derived by referring to an infinite planar surface with the same tensor impedance of the pertinent face of the wedge. As far as the second-order correction to the field is concerned, the residue contributions associated with geometrical poles are

$$\begin{aligned}&\mathrm{Res}\{f_2(\alpha+\phi-n\pi/2)e^{jk_t\rho\,\cos\,\alpha},\ \alpha=\alpha_{0,n}^{go}\}\\ &\quad=\left(-\frac{2\,\cos\,\xi_{0,n}}{\sin\,\xi_{0,n}+\sin\,\theta_{0,n}^{h}}+\sin\,\theta_{0,n}^{e}\right)\\ &\qquad\cdot\frac{\sin\,\xi_{0,n}e^{jk_t\rho\,\cos\,a_{0,n}^{go}}}{(\sin\,\xi_{0,n}+\sin\,\theta_{0,n}^{e})^2}\end{aligned} \tag{19}$$

$$\begin{aligned}&\mathrm{Res}\{s_2(\alpha+\phi-n\pi/2)e^{jk_t\rho\,\cos\,\alpha},\ \alpha=\alpha_{0,n}^{go}\}\\ &\quad=\left(-\frac{2\,\cos\,\xi_{0,n}}{\sin\,\xi_{0,n}+\sin\,\theta_{0,n}^{e}}+\sin\,\theta_{0,n}^{h}\right)\\ &\qquad\cdot\frac{\sin\,\xi_{0,n}e^{jk_t\rho\,\cos\,\alpha_{0,n}^{go}}}{(\sin\,\xi_{0,n}+\sin\theta_{0,n}^{h})^2}.\end{aligned} \tag{20}$$

It is worth observing that the locations of these latter geometrical poles are the same as those of the first-order corrections in (17) and (18); again, their residue contributions must be taken into account when $0 < (\epsilon_{0,n}+1)n\pi/2 - \epsilon_{0,n}\phi < \pi - \xi_{0,n}$. We note that the residue expressions in (19) and (20) coincide with one half of the second-order derivative with respect to $\cos\,\beta'$ of the diagonal terms in the reflection matrix of the corresponding anisotropic wedge face, evaluated at $\beta' = \pi/2$.

2) Electric Poles: Electric poles are identified with the poles of the Maliuzhinets special function $\Psi^{e,h}(\alpha)$ and, in part, with the poles of the function $[\sigma_m(\alpha),\, \tau_m(\alpha)]$, $m = 1, 2$. Their locations on the complex α plane are

$$\alpha = \alpha_2 = \alpha_{0,n}^{e} = -\phi + n\pi/2 + \epsilon_{0,n}(\pi + \theta_{0,n}^{e} + n\pi/2) \tag{21}$$

$$\alpha = \alpha_3 = \alpha_{0,n}^{h} = -\phi + n\pi/2 + \epsilon_{0,n}(\pi + \theta_{0,n}^{h} + n\pi/2). \tag{22}$$

The corresponding expressions for the residue contributions are as shown in (23)–(26), given at the bottom of the next page. They must be included in the solution when $0 < (\epsilon_{0,n}+1)n\pi/2 - \epsilon_{0,n}\phi < \mathrm{gd}\{\Im(\theta_{0,n}^{e})\} - \Re(\theta_{0,n}^{e})$ and $0 < (\epsilon_{0,n}+1)n\pi/2 - \epsilon_{0,n}\phi < \mathrm{gd}\{\Im(\theta_{0,n}^{h})\} - \Re(\theta_{0,n}^{h})$. As far as $[f_2,\, s_2]$ are concerned, they exhibit second-order pole singularities at $\alpha = \alpha_2,\, \alpha_3$. For the sake of simplicity, their residues have not been taken into account in the asymptotic evaluation. However, we note that their contribution is of order $\cos^2\,\beta'$ in our perturbative solution and provide corrections to the surface wave contributions (when they exist) so that their influence is confined to the neighborhoods of the faces of the wedge.

B. Contributions of the SDP Integrals

In order to obtain suitable high-frequency expressions, the integrals along the SDP's are asymptotically evaluated by retaining all terms of order $(k_t\rho)^{-1/2}$ as suggested in [20], so that the crossing of a pole through the SDP's is properly

accounted for, also when this crossing takes place away from saddle points, as for instance in the case of the surface wave poles. This yields a uniform high-frequency solution for the diffracted field contribution, which is given next in a compact matrix form

$$\begin{bmatrix} E_z^d \\ \zeta_0 H_z^d \end{bmatrix} = \begin{bmatrix} D_{ee} & D_{eh} \\ D_{he} & D_{hh} \end{bmatrix} \begin{bmatrix} e_z \\ h_z \end{bmatrix} \tag{27}$$

where

$$D_{ee} = D_{ee}^{(0)} + \cos^2 \beta' D_{ee}^{(2)} \tag{28a}$$
$$D_{hh} = D_{hh}^{(0)} + \cos^2 \beta' D_{hh}^{(2)} \tag{28b}$$
$$D_{eh} = \cos \beta' D_{eh}^{(1)} \tag{28c}$$
$$D_{he} = \cos \beta' D_{he}^{(1)}. \tag{28d}$$

In particular

$$D_{eh}^{(1)} = -\frac{e^{-j\pi/4}e^{-jk_t\rho}}{\sqrt{2\pi k_t\rho}} \cdot \left\{ f_1(\pi+\phi-n\pi/2) - f_1(-\pi+\phi-n\pi/2) - \sum_{i=1}^{3} \mathrm{Res}\{f_1(\alpha+\phi-n\pi/2),\, \alpha=\alpha_i\} \cdot \frac{1-\mathbb{F}\left[\sqrt{k_t\rho(1+\cos\,\alpha_i)}\right]}{2\,\cos(\alpha_i/2)} \right\} \tag{29}$$

$$D_{he}^{(1)} = -\frac{e^{-j\pi/4}e^{-jk_t\rho}}{\sqrt{2\pi k_t\rho}} \cdot \left\{ s_1(\pi+\phi-n\pi/2) - s_1(-\pi+\phi-n\pi/2) - \sum_{i=1}^{3} \mathrm{Res}\{s_1(\alpha+\phi-n\pi/2),\, \alpha=\alpha_i\} \cdot \frac{1-\mathbb{F}\left[\sqrt{k_t\rho(1+\cos\,\alpha_i)}\right]}{2\,\cos(\alpha_i/2)} \right\} \tag{30}$$

$$D_{ee}^{(2)} = -\frac{e^{-j\pi/4}e^{-jk_t\rho}}{\sqrt{2\pi k_t\rho}} \cdot \left\{ f_2(\pi+\phi-n\pi/2) - f_2(-\pi+\phi-n\pi/2) - \mathrm{Res}\{f_2(\alpha+\phi-n\pi/2),\, \alpha=\alpha_1\} \cdot \frac{1-\mathbb{F}\left[\sqrt{k_t\rho(1+\cos\,\alpha_1)}\right]}{2\,\cos(\alpha_1/2)} \right\} \tag{31}$$

$$D_{hh}^{(2)} = -\frac{e^{-j\pi/4}e^{-jk_t\rho}}{\sqrt{2\pi k_t\rho}} \cdot \left\{ s_2(\pi+\phi-n\pi/2) - s_2(-\pi+\phi-n\pi/2) - \mathrm{Res}\{s_2(\alpha+\phi-n\pi/2),\, \alpha=\alpha_1\} \cdot \frac{1-\mathbb{F}\left[\sqrt{k_t\rho(1+\cos\,\alpha_1)}\right]}{2\,\cos(\alpha_1/2)} \right\}. \tag{32}$$

In the previous equations, $\mathbb{F}(z)$ is the UTD transition function generalized to complex arguments as in [20]. Suitable uniform asymptotic expressions for $D_{ee}^{(0)}$ and $D_{hh}^{(0)}$ are given in [19], with $k\rho$ substituted by $k_t\rho$.

Finally, we observe that the copolar components in (27) depend only on even powers of $\cos\,\beta'$, while the cross-polar components depend on odd powers. This remains true also including other higher order terms, as directly follows from the considerations done in Appendix A. This also implies that including terms up to the second order in $\cos\,\beta'$ in (6) leads to errors of order $\cos^4\,\beta'$ and $\cos^3\,\beta'$ for the copolar and cross-polar components of the fields, respectively.

V. Numerical Results

Samples of numerical results are presented in this section in order to validate the technique proposed and to discuss its limits of applicability. The results have been compared with those obtained by reference solutions presented in the literature both for isotropic and anisotropic impedance wedges at skew incidence. In all the examples presented, we refer to the case

$$\mathrm{Res}\{f_1(\alpha+\phi-n\pi/2)e^{jk_t\rho\,\cos\,\alpha},\, \alpha=\alpha_{0,n}^e\} = \mathrm{Res}\{\Psi^e(\alpha+\phi-n\pi/2),\, \alpha=\alpha_{0,n}^e\}\tau_1(\alpha_{0,n}^e+\phi-n\pi/2)e^{jk_t\rho\,\cos\,\alpha_{0,n}^e} \tag{23}$$

$$\mathrm{Res}\{s_1(\alpha+\phi-n\pi/2)e^{jk_t\rho\,\cos\,\alpha},\, \alpha=\alpha_{0,n}^h\} = \mathrm{Res}\{\Psi^h(\alpha+\phi-n\pi/2),\, \alpha=\alpha_{0,n}^h\}\sigma_1(\alpha_{0,n}^h+\phi-n\pi/2)e^{jk_t\rho\,\cos\,\alpha_{0,n}^h} \tag{24}$$

$$\mathrm{Res}\{f_1(\alpha+\phi-n\pi/2)e^{jk_t\rho\,\cos\,\alpha},\, \alpha=\alpha_{0,n}^h\} = \epsilon_{0,n}e^{jk_t\rho\,\cos\,\alpha_{0,n}^h}\,\frac{\cos\,\theta_{0,n}^h\,\mathrm{Res}\{\Psi^h(\alpha+\phi-n\pi/2),\, \alpha=\alpha_{0,n}^h\}\sigma(\alpha_{0,n}^h+\phi-n\pi/2)}{(\sin\,\theta_{0,n}^h-\sin\,\theta_{0,n}^e)\Psi^h(\phi'-n\pi/2)} \tag{25}$$

$$\mathrm{Res}\{s_1(\alpha+\phi-n\pi/2)e^{jk_t\rho\,\cos\,\alpha},\, \alpha=\alpha_{0,n}^e\} = -\epsilon_{0,n}e^{jk_t\rho\,\cos\,\alpha_{0,n}^e}\,\frac{\cos\,\theta_{0,n}^e\,\mathrm{Res}\{\Psi^e(\alpha+\phi-n\pi/2),\, \alpha=\alpha_{0,n}^e\}\sigma(\alpha_{0,n}^e+\phi-n\pi/2)}{(\sin\,\theta_{0,n}^e-\sin\,\theta_{0,n}^h)\Psi^e(\phi'-n\pi/2)} \tag{26}$$

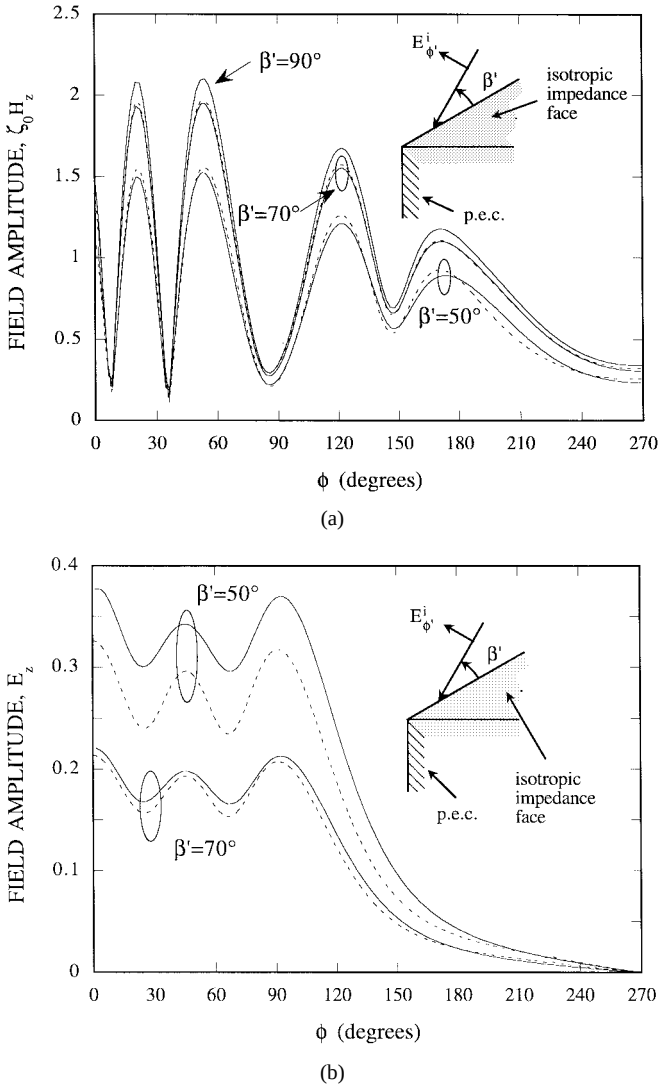

Fig. 3. Amplitude of the (a) copolar and (b) cross-polar longitudinal components of the total field in the presence of a right-angled isotropic impedance wedge with $(Z_0)_z/\zeta_0 = (Z_0)_\rho/\zeta_0 = j/2$, $(Z_n)_z = (Z_n)_\rho = 0$. Geometrical and electrical parameters: $n = 3/2$, $\phi' = 45°$, $\beta' = 50, 70, 90°$, $k_t\rho = 10$, $E^i_{\beta'} = 0$, $E^i_{\phi'} = 1$. This solution: zeroth- and first-order contributions for copolar and cross-polar components, respectively (dashed lines); asymptotic evaluation of the analytical solution in [15] (solid lines).

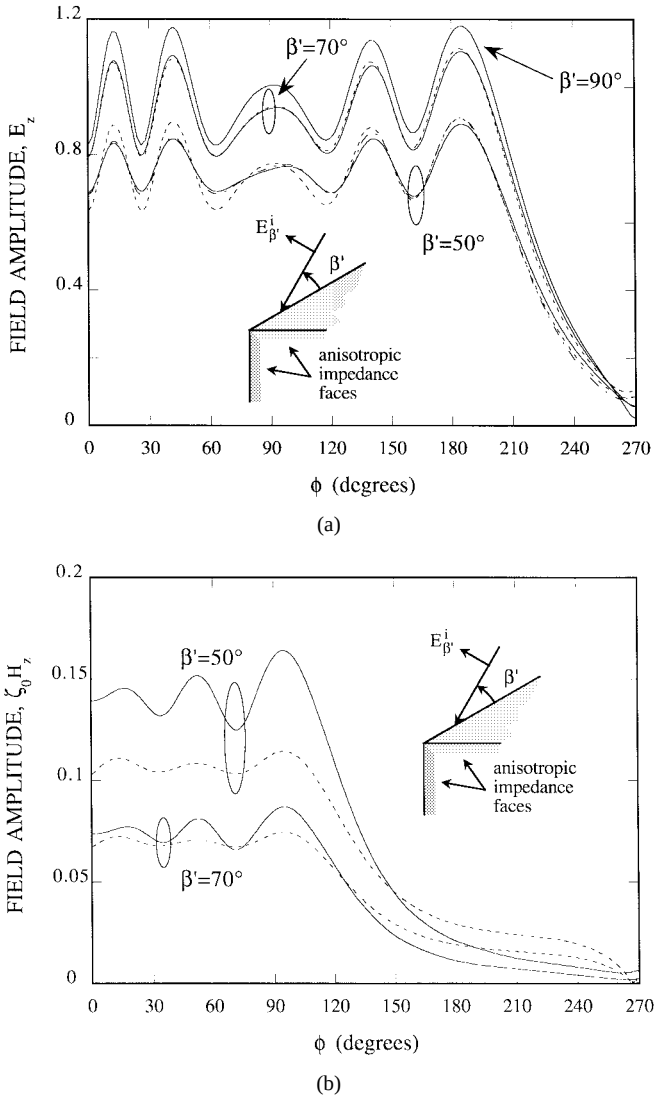

Fig. 4. Amplitude of the (a) copolar and (b) cross-polar longitudinal components of the total field in the presence of a right-angled anisotropic impedance wedge with $(Z_{0,n})_z/\zeta_0 = 1$, $(Z_{0,n})_\rho/\zeta_0 = 2$. Geometrical and electrical parameters: $n = 3/2$, $\phi' = 45°$, $\beta' = 50, 70, 90°$, $k_t\rho = 10$, $E^i_{\beta'} = 1$, $E^i_{\phi'} = 0$. This solution: zeroth- and first-order contributions for copolar and cross-polar components, respectively (dashed lines); parabolic equation method [2] (solid lines); Maliuzhinets solution (solid line, $\beta' = 90°$); this solution augmented by second-order term (dashed–dotted line, $\beta' = 50°$).

of a right-angled wedge ($n = 3/2$)—this choice is motivated by the fact that for this configuration the Maliuzhinets special function is known in a simple closed form [14], [17].

Comparisons between data relevant to the amplitude of copolar and cross-polar components of the total field, obtained by this approximated method (dashed lines) and calculated by the uniform asymptotic expressions in [15] (continuous lines), are shown in Fig. 3(a) and (b), respectively, for a right-angled isotropic impedance wedge with $(Z_0)_z/\zeta_0 = (Z_0)_\rho/\zeta_0 = j/2$ and $(Z_n)_z = (Z_n)_\rho = 0$ (the face $\phi = 3\pi/2$ is perfectly conducting). In the example shown, $\phi' = 45°$, $k_t\rho = 10$, and β' is assumed as a parameter, with $\beta' = 50, 70°$. The incident plane wave is linearly polarized with $E^i_{\beta'} = 0$, $E^i_{\phi'} = 1$ in the standard ray-fixed ray coordinate system [12] (TE_z polarization). A reference curve, obtained by evaluating the asymptotic approximation of the Maliuzhinets solution [19], valid at normal incidence $\beta' = 90°$, is also plotted in Fig. 3(a) to highlight the effects introduced by the variation of the incidence skewness angle β'. It is important to note that the data in Fig. 3(a), both for $\beta' = 70°$ and $\beta' = 50°$, have been calculated by including just the zeroth-order term, obtaining a good agreement with the reference solution up to $\beta' = 50°$. A good agreement is also observed for the cross-polar component in Fig. 3(b) up to $\beta' = 70°$.

A further example is shown in Fig. 4. Here, the right-angled wedge is characterized by two anisotropic impedance faces, with $(Z_{0,n})_z/\zeta_0 = 1$, $(Z_{0,n})_\rho/\zeta_0 = 2$. The incident plane wave is TM_z polarized ($E^i_{\beta'} = 1$, $E^i_{\phi'} = 0$) and impinges from $\phi' = 45°$, $\beta' = 50, 70, 90°$—the field is evaluated at $k_t\rho = 10$. In particular, curves for the amplitude of both the copolar (E_z) and cross-polar ($\zeta_0 H_z$) longitudinal

components of the total field are plotted in Fig. 4(a) and (b), respectively. They have been calculated by this approximate solution (dashed lines), including only the zeroth- and the first-order term, respectively, and compared with the results obtained by the parabolic equation method (solid lines) [2]. Again, the reference curve corresponding to $\beta' = 90°$ in Fig. 4(a), has been determined by means of the asymptotic evaluation of the Maliuzhinets two-dimensional (2-D) solution. To demonstrate the convergence of the approximate solution, a further curve which includes the contribution of the second-order correction to the field (dashed–dotted line) has been plotted in Fig. 4(a) for the case $\beta' = 50°$—as apparent, the accuracy of the approximate predictions is augmented by the introduction of the second-order contribution.

Curves for both the copolar (E_z) and cross-polar ($\zeta_0 H_z$) longitudinal components of the total field in the presence of an impedance right-angled wedge, with the zero-face anisotropic $(Z_0)_z/\zeta_0 = 1$, $(Z_0)_\rho = 0$, and the n-face isotropic $(Z_n)_z/\zeta_0 = (Z_n)_\rho/\zeta_0 = j/2$, are plotted in Fig. 5(a) and (b), respectively. The wedge is illuminated by a TM_z polarized plane wave ($E^i_{\beta'} = 1$, $E^i_{\phi'} = 0$), impinging on the edge from $\phi' = 30°$ and $\beta' = 50, 70, 90°$. The field is evaluated at $k_t\rho = 10$. Curves calculated through this approximate solution (dashed line), evaluated by including just the zeroth-order term in Fig. 5(a) and the first-order term in Fig. 5(b), are compared with those obtained by the UTD asymptotic evaluation of the exact solution given in [10] (solid line). A further curve (dashed–dotted line), obtained by adding the second-order contribution to the copolar longitudinal component, is plotted in Fig. 5(a) for $\beta' = 50°$—as apparent, the accuracy of the results is improved. Moreover, Fig. 5(b) shows that the first-order correction to the field properly fits the rapidly varying behavior of the total field in the neighborhoods of the isotropic impedance $\phi = 3\pi/2$ face, which is due to the excitation of surface waves on the same face.

The case of a right-angled wedge with anisotropic impedance faces, characterized by a vanishing impedance in the direction of the edge $(Z_0)_z = 0$, $(Z_0)_\rho/\zeta_0 = (1+j)/2$, $(Z_n)_z = 0$, $(Z_n)_\rho/\zeta_0 = (1-j)/2$, is analyzed next. The incident plane wave is TE_z polarized ($E^i_{\beta'} = 0$, $E^i_{\phi'} = 1$) and impinges from a set of directions identified by $\phi' = 30°$ and $\beta' = 50, 70, 90°$. In particular, plots for the amplitude of the copolar component ($\zeta_0 H_z$) of the total field, evaluated at $k_t\rho = 10$, are shown in Fig. 6, where data obtained by the zeroth-order approximation of this solution (dashed lines) are compared with those calculated by a uniform asymptotic approximation of the exact solution in [9] (solid lines). Again, to check the convergence of the procedure also a curve obtained by improving this approximate solution with the second-order contribution (dashed–dotted line) is plotted—as apparent, a better agreement is obtained in this latter case also at $\beta' = 50°$. Finally, it is worth noting that, in the specific case $(Z_{0,n})_z = 0$, the boundary conditions at both faces of the wedge are decoupled when expressed in terms of the longitudinal components of the fields [9], so that the cross-polar longitudinal component is identically zero. Moreover, for TM_z plane wave illumination ($E^i_{\beta'} = 1$, $E^i_{\phi'} = 0$) the E_z component of the total field reduces to the solution for the perfectly conducting wedge, which is recovered by the only zeroth-order term in this approximate representation.

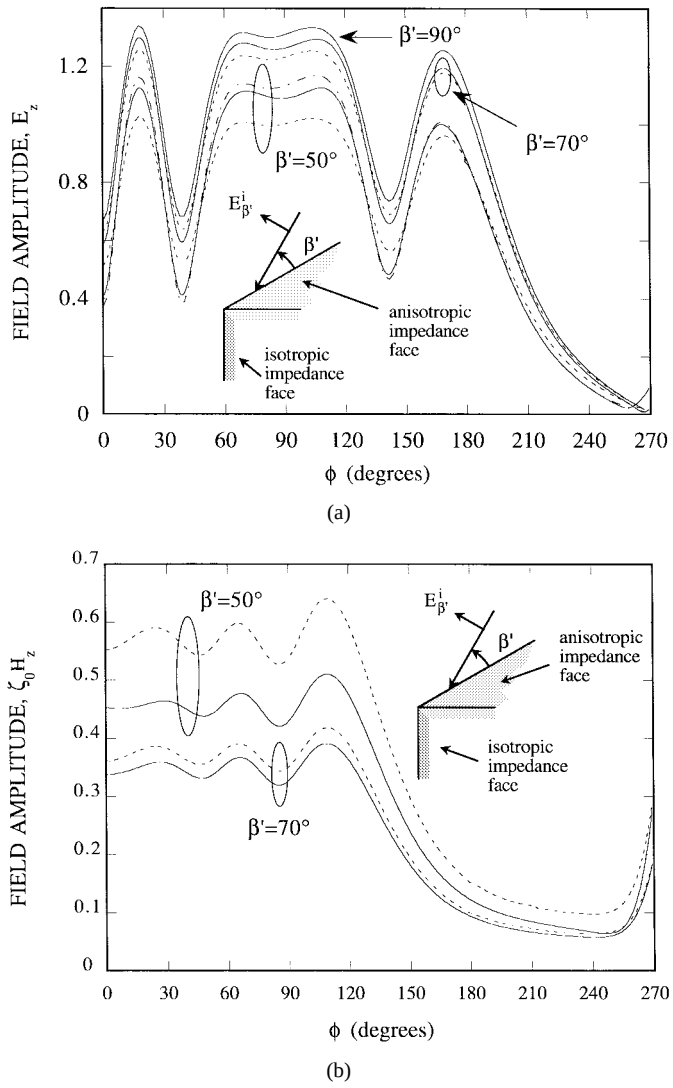

Fig. 5. Amplitude of the (a) copolar and (b) cross-polar longitudinal components of the total field in the presence of a right-angled anisotropic impedance wedge with $(Z_0)_z/\zeta_0 = 1$, $(Z_0)_\rho/\zeta_0 = 0$, $(Z_n)_z/\zeta_0 = (Z_n)_\rho/\zeta_0 = j/2$. Geometrical and electrical parameters: $n = 3/2$, $\phi' = 30°$, $\beta' = 50, 70, 90°$, $k_t\rho = 10$, $E^i_{\beta'} = 1$, $E^i_{\phi'} = 0$. This solution: zeroth- and first-order contributions for copolar and cross-polar components, respectively (dashed lines); UTD solution [10] (solid lines); this solution augmented by the second-order term (dashed–dotted line, $\beta' = 50°$).

Extended numerical tests have shown that this approximate high-frequency solution provides accurate results far beyond the standard limits of applicability of perturbative methods ($\cos\beta' < 0.1$). As demonstrated also by the numerical examples shown here, errors of a few percents are obtained for the copolar components up to $\beta' = 70°$ when just the zeroth-order term is taken into account. This limit can be extended to $\beta' = 50°$ when also the second term is included in the calculations—this implies neglecting $O(\cos^4\beta')$. As far as cross-polar components are concerned, accounting for the only first-order term—this implies neglecting $O(\cos^3\beta')$—guarantees an error less then 10% up to $\beta' = 70°$. This higher percent error is due to the fact that the amplitude of the cross-polar component close to normal incidence is approximately

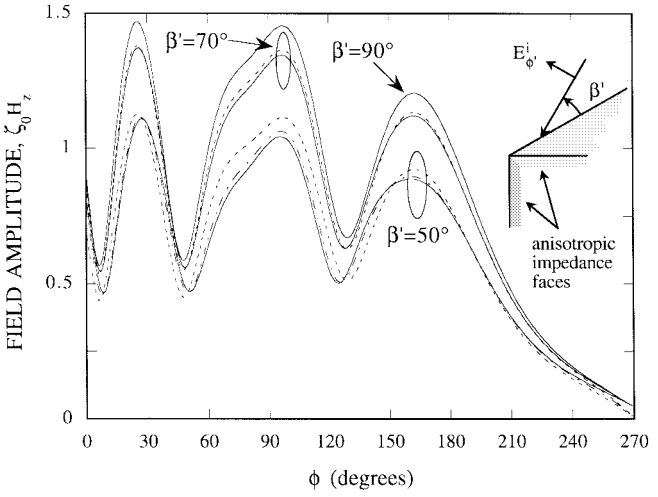

Fig. 6. Amplitude of the copolar longitudinal component of the total field in the presence of a right-angled anisotropic impedance wedge with $(Z_0)_z = 0$, $(Z_0)_\rho/\zeta_0 = (1+j)/2$, $(Z_n)_z = 0$, $(Z_n)_\rho/\zeta_0 = (1-j)/2$. Geometrical and electrical parameters: $n = 3/2$, $\phi' = 30°$, $\beta' = 50, 70, 90°$, $k_t\rho = 10$, $E^i_{\beta'} = 0$, $E^i_{\phi'} = 1$. This solution zeroth-order (dashed lines); UTD solution [9] (solid lines); this solution augmented by the second-order term (dashed–dotted line, $\beta' = 50°$).

an order of magnitude lower than that of the corresponding copolar component.

VI. Conclusions

Uniform approximate asymptotic expressions for the fields scattered from an anisotropic impedance wedge, illuminated by an arbitrarily polarized plane wave impinging on the edge at oblique incidence, have been provided in the UTD format. The specific surface impedance tensors defined on the two faces of the wedge have their principal axes parallel and perpendicular to the edge. The asymptotic formulas are obtained by resorting to a perturbative approach and are valid for deviations from the normal incidence case which in general are of the order of 20° to 30° ($\beta' = 70°$ to $60°$). The limits of applicability of the expressions derived have been determined by performing extended numerical tests and comparing the results with those derived from reference solutions available in the literature. Finally, it is worth noting that the isotropic impedance wedge case is contained as a limit in the analysis proposed.

Appendix A

The main purpose of this Appendix is to justify the specific form given in (6) for the spectral functions. For obtaining a solution of the functional equations in (5), we can assume the following series expansions for $f(\alpha)$ and $s(\alpha)$:

$$f(\alpha) = \sum_{m=0}^{\infty} F_m(\alpha)\ \cos^m\ \beta' \tag{A.1a}$$

$$s(\alpha) = \sum_{m=0}^{\infty} S_m(\alpha)\ \cos^m\ \beta'. \tag{A.1b}$$

On substituting the above expressions into (5) and equating the coefficients of like powers of $\cos\ \beta'$, a recursive system is obtained

$$\begin{aligned}&(\sin\ \alpha + \epsilon_{0,n}\ \sin\ \beta'\ \sin\ \theta^e_{0,n})F_m(\alpha + \epsilon_{0,n}n\pi/2)\\ &\quad + (\sin\ \alpha - \epsilon_{0,n}\ \sin\ \beta'\ \sin\ \theta^e_{0,n})F_m(-\alpha + \epsilon_{0,n}n\pi/2)\\ &\quad = \cos\ \alpha\{S_{m-1}(\alpha + \epsilon_{0,n}n\pi/2)\\ &\qquad - S_{m-1}(-\alpha + \epsilon_{0,n}n\pi/2)\}\end{aligned} \tag{A.2a}$$

$$\begin{aligned}&(\sin\ \alpha + \epsilon_{0,n}\ \sin\ \beta'\ \sin\ \theta^h_{0,n})S_m(\alpha + \epsilon_{0,n}n\pi/2)\\ &\quad + (\sin\ \alpha - \epsilon_{0,n}\ \sin\ \beta'\ \sin\ \theta^h_{0,n})S_m(-\alpha + \epsilon_{0,n}n\pi/2)\\ &\quad = \cos\ \alpha\{F_{m-1}(\alpha + \epsilon_{0,n}n\pi/2)\\ &\qquad - F_{m-1}(-\alpha + \epsilon_{0,n}n\pi/2)\}\end{aligned} \tag{A.2b}$$

where $S_{-1}(\alpha) = F_{-1}(\alpha) = 0$. It is apparent that the functional equations for $F_0(\alpha)$ and $S_0(\alpha)$ are decoupled so that the same functions are proportional to the amplitude of the incident electric and magnetic field longitudinal components, respectively

$$F_0(\alpha) = e_z f_0(\alpha) \tag{A.3a}$$

$$S_0(\alpha) = h_z s_0(\alpha). \tag{A.3b}$$

Consequently, the structure of the recursive system implies that $F_m(\alpha)$ and $S_m(\alpha)$, for m even, are proportional to the incident electric (e_z) and magnetic (h_z) field longitudinal components, respectively. On the contrary, $F_m(\alpha)$ and $S_m(\alpha)$, for m odd, are proportional to h_z and e_z, respectively. As a consequence the total electric field longitudinal component consists of two contributions. The first one is proportional to e_z (copolar contribution) and results to be an even function of $\cos\ \beta'$; the second is proportional to h_z (cross-polar contribution) and results to be an odd function of $\cos\ \beta'$. By duality, similar considerations are valid for the total magnetic field longitudinal component.

Appendix B

In order to evaluate $[f_{1,2}(\alpha),\ s_{1,2}(\alpha)]$ suitable expressions for $[\tau_{1,2}(\alpha),\ \sigma_{1,2}(\alpha)]$ are needed. By substituting (13a) and (13b) into (9) and (12), respectively, it is found that $[\tau_{1,2}(\alpha),\ \sigma_{1,2}(\alpha)]$ must satisfy the following inhomogeneous functional equations:

$$\begin{aligned}&[\tau_1(\alpha^+_{0,n}),\ \sigma_1(\alpha^+_{0,n})] - [\tau_1(\alpha^-_{0,n}),\ \sigma_1(\alpha^-_{0,n})]\\ &\quad [K^e_{0,n}(\alpha),\ K^h_{0,n}(\alpha)]\end{aligned} \tag{B.1}$$

$$\begin{aligned}&[\tau_2(\alpha^+_{0,n}),\ \sigma_2(\alpha^+_{0,n})] - [\tau_2(\alpha^-_{0,n}),\ \sigma_2(\alpha^-_{0,n})]\\ &\quad [H^e_{0,n}(\alpha),\ H^h_{0,n}(\alpha)].\end{aligned} \tag{B.2}$$

In (B.1)

$$K^e_{0,n}(\alpha) = \frac{L_{0,n}(\alpha,\ \theta^e_{0,n};\ s_0)}{\Psi^e(\alpha^+_{0,n})} \tag{B.3a}$$

$$K^h_{0,n}(\alpha) = \frac{-L_{0,n}(\alpha,\ \theta^h_{0,n};\ f_0)}{\Psi^h(\alpha^+_{0,n})} \tag{B.3b}$$

and in (B.2)

$$H^{e}_{0,n}(\alpha) = \frac{1}{\Psi^{e}(\alpha^{+}_{0,n})}\left\{ L_{0,n}(\alpha,\, \theta^{e}_{0,n};\, s_1) + \epsilon_{0,n}\, \frac{\sin\, \theta^{e}_{0,n}}{2\, \cos\, \alpha} \cdot\, L_{0,n}(\alpha,\, \theta^{e}_{0,n};\, f_0) \right\} \tag{B.4a}$$

$$H^{h}_{0,n}(\alpha) = \frac{1}{\Psi^{h}(\alpha^{+}_{0,n})}\left\{ -L_{0,n}(\alpha,\, \theta^{h}_{0,n};\, f_1) + \epsilon_{0,n}\, \frac{\sin\, \theta^{h}_{0,n}}{2\, \cos\, \alpha} \cdot\, L_{0,n}(\alpha,\, \theta^{h}_{0,n};\, s_0) \right\}. \tag{B.4b}$$

The solution of (B.1) and (B.2) has been given by Tuzhilin in [18], in the form of special integral functions, with the integrals defined along the imaginary axis of the complex plane. We can write

$$\tau_{1,2}(\alpha) = \tau^{0}_{1,2}(\alpha) + \tau^{n}_{1,2}(\alpha) \tag{B.5}$$

$$\sigma_{1,2}(\alpha) = \sigma^{0}_{1,2}(\alpha) + \sigma^{n}_{1,2}(\alpha) \tag{B.6}$$

with

$$[\tau^{0,n}_{1},\, \sigma^{0,n}_{1}] = -\frac{j}{4n\pi} \int_{-j\infty}^{+j\infty} [K^{e}_{0,n}(\xi),\, K^{h}_{0,n}(\xi)] \cdot \mathrm{tg}\left(\frac{\alpha + \epsilon_{0,n} n\pi/2 - \xi}{2n} \right) d\xi \tag{B.7}$$

$$[\tau^{0,n}_{2},\, \sigma^{0,n}_{2}] = -\frac{j}{4n\pi} \int_{-j\infty}^{+j\infty} [H^{e}_{0,n}(\xi),\, H^{h}_{0,n}(\xi)] \cdot \mathrm{tg}\left(\frac{\alpha + \epsilon_{0,n} n\pi/2 - \xi}{2n} \right) d\xi. \tag{B.8}$$

The previous definitions for $[\tau^{0}_{1,2}(\alpha),\, \sigma^{0}_{1,2}(\alpha)]$ and $[\tau^{n}_{1,2}(\alpha),\, \sigma^{n}_{1,2}(\alpha)]$ are valid in the strips $-n\pi/2 < \Re(\alpha) < 3n\pi/2$ and $-3n\pi/2 < \Re(\alpha) < n\pi/2$, respectively. Outside these regions, an analytic continuation is required [18], which is based on the functional equations in (B.1) and (B.2).

It can be shown that $[K^{e}_{0,n}(\xi),\, K^{h}_{0,n}(\xi)]$ and $[H^{e}_{0,n}(\xi),\, H^{h}_{0,n}(\xi)]$ are odd functions; their amplitude tends to zero exponentially when $\mathrm{Im}(\xi) \to \pm\infty$. This renders the integrals in (B.7) and (B.8) rapidly convergent. However, it is worth noting that the computational complexity significantly increases when the evaluation of second-order contribution is required. Indeed, the integrand in (B.8) implicitly contains the integral in (B.7), so that a double integration is involved.

REFERENCES

[1] J. H. Bilow, "Scattering by an infinite wedge with tensor impedance boundary conditions—A moment method/physical optics solution for the currents," *IEEE Trans. Antennas Propagat.*, vol. 39, no. 6, pp. 767–773, 1992.

[2] G. Pelosi, S. Selleri, and R. D. Graglia, "The parabolic equation model for the numerical analysis of the diffraction at an anisotropic impedance wedge," *IEEE Trans. Antennas Propagat.*, vol. 45, no. 5, pp. 767–771, 1997.

[3] N. Y. Zhu and F. M. Landstofer, "Numerical study of diffraction and slope-diffraction at anisotropic impedance wedges by the method of parabolic equation: Space waves," *IEEE Trans. Antennas Propagat.*, vol. 45, no. 5, pp. 822–828, 1997.

[4] Y. I. Nefedov and A. T. Fialkovskiy, "Diffraction of plane electromagnetic wave at anisotropic half-plane in free space and in planar waveguide," *Radio Eng. Electron. Phy.*, vol. 17, no. 6, pp. 887–896, 1972.

[5] T. B. A. Senior, "Some problems involving imperfect half-planes," in *Electromagnetic Scattering*, P. L. E. Uslenghi, Ed. New York: Academic, 1978, pp. 185–219.

[6] A. H. Serbest, A. Buyukaksoy, and G. Uzgoren, "Diffraction by a discontinuity formed by two anisotropic impedance half planes," *Trans. IEICE*, vol. E-74, pp. 1283–1287, May 1991.

[7] M. A. Lyalinov, "Diffraction by a wedge with anisotropic face impedances," *Ann. Télécommun.*, vol. 49, no. 11/12, pp. 667–672, 1994.

[8] ———, "On one approach to an electromagnetic diffraction problem in a wedge shaped region," *J. Phys. A Math. Gen.*, vol. 27, pp. L183–L189, 1994.

[9] G. Manara, P. Nepa, and G. Pelosi, "A UTD solution for plane wave diffraction at an edge in an artificially hard surface: Oblique incidence case," *Electron. Lett.*, vol. 31, no. 19, pp. 1649–1650, 1995.

[10] ———, "Electromagnetic scattering by a right-angled anisotropic impedance wedge," *Electron. Lett.*, vol. 32, no. 13, pp. 1179–1180, 1996.

[11] P. Nepa, G. Manara, and G. Pelosi, "A UTD solution for the diffraction at an edge in a planar anisotropic impedance surface: Oblique incidence case," *Microwave Opt. Technol. Lett.*, vol. 9, no. 5, pp. 55–59, Oct. 1996.

[12] R. G. Kouyoumjian and P. H. Pathak, "A uniform geometrical theory of diffraction for an edge in a perfectly conducting surface," *Proc. IEEE*, vol. 62, pp. 1448–1461, Nov. 1974.

[13] G. Pelosi, G. Manara, and P. Nepa, "Diffraction by a wedge with variable impedance walls," *IEEE Trans. Antennas Propagat.*, vol. 44, no. 10, pp. 1334–1340, 1996.

[14] G. D. Maliuzhinets, "Excitation, reflection and emission of surface waves from a wedge with given face impedances," *Sov. Phys. Dokl.*, vol. 3, pp. 752–755, 1958.

[15] R. G. Rojas, "Electromagnetic diffraction of an obliquely incident plane wave field by a wedge with impedance faces," *IEEE Trans. Antennas Propagat.*, vol. 36, no. 7, pp. 956–970, 1988.

[16] G. D. Maliuzhinets, "Inversion formula for the Sommerfeld integral," *Sov. Phys. Dokl.*, vol. 3, pp. 52–56, 1958.

[17] T. B. A. Senior and J. L. Volakis, *Approximate Boundary Conditions in Electromagnetics*. London, U.K.: IEE, 1995.

[18] A. A. Thuzhilin, "The theory of Maliuzhinets inhomogeneous functional equations," *Differ. Urav.*, vol. 9, pp. 2058–2064, 1973.

[19] R. Tiberio, G. Pelosi, and G. Manara, "A uniform GTD formulation for the diffraction by a wedge with impedance faces," *IEEE Trans. Antennas Propagat.*, vol. AP-33, no. 8, pp. 867–872, 1985.

[20] R. G. Kouyoumjian, G. Manara, P. Nepa, and B. J. E. Taute, "The diffraction of an inhomogeneous plane wave by a wedge," *Radio Sci.*, vol. 31, no. 6, pp. 1387–1398, Nov./Dec. 1996.

Giuseppe Pelosi (M'88–SM'91) was born in Pisa, Italy, on December 25, 1952. He received the Laurea (Doctor) degree in physics (*summa cum laude*) from the University of Florence in 1976.

Since 1979, he has been with the Department of Electrical Engineering, University of Florence, where he is currently an Associate Professor of Microwave Engineering. He has been mainly involved in research in the field of numerical and asymptotic techniques for applied electromagnetics. His research interests included extensions and applications of the geometrical theory of diffraction as well as methods for radar cross-section analysis of complex targets. His current research activity is mainly devoted to the development of numerical procedures in the context of the finite-element method, with particular emphasis on radiation and scattering problems. He is a coauthor of three books: *Finite Elements for Wave Propagation* (New York: IEEE, 1994), *Finite Element Software for Microwave Engineering* (New York: Wiley, 1996), and *Quick Finite Element Method for Electromagnetic Waves* (Norwood, MA: Artech House, 1998).

Dr. Pelosi is a Member of the Applied Computational Electromagnetics Society.

Giuliano Manara (M'88–SM'93) was born in Florence, Italy, on October 30, 1954. He received the Laurea (Doctor) degree in electronics engineering (*summa cum laude*) from the University of Florence, Italy, in 1979.

He was first with the Department of Electrical Engineering, University of Florence, as a Postdoctoral Research Fellow. Then, in 1987 he joined the Department of Information Engineering, University of Pisa, where he works presently as an Associate Professor. Since 1980, he has been collaborating with the Department of Electrical Engineering, Ohio State University, Columbus, where in summer and fall of 1987 he was involved in research at the Electro Science Laboratory. His current research interests include radar systems, numerical and asymptotic techniques in electromagnetic scattering, and radiation problems.

Dr. Manara is a Member of the Italian Electrical and Electronic Engineers Association (AEI).

Paolo Nepa (M'95) was born in Teramo, Italy, on August 7, 1965. He received the Laurea (Doctors) degree in electronics engineering (*summa cum laude*) from the University of Pisa, Pisa, Italy, in 1990.

He joined the Department of Information Engineering, University of Pisa, where he is presently an Assistant Professor. His current research interests include the development and application of uniform asymptotic techniques in electromagnetic scattering.